PAPER

Check for updates

First thermal studies on visible-light-switchable negative T-type photochromes of a nitrile-rich series†

Mikhail Yu. Belikov ID * and Mikhail Yu. Ievlev ID

Representatives of visible-light-switchable nitrile-rich negative T-type photochromes (**NRP**) were synthesized. The temperature effect on the thermal relaxation of the photoinduced form of **NRP** was studied for the first time. It was found that regardless the temperature the reverse thermal reaction in ethanol and 1,4-dioxane proceeded according to a first-order kinetic equation, while an unusual pseudo-zero order of the dark reaction was observed in acetonitrile. Using the obtained experimental data, the activation energy as well as the activation parameters, such as entropy and enthalpy of activation, were calculated for the first time for thermal relaxation of **NRP** photochromes. It was also shown that an initial form of **NRP** photochromes bearing a tricyanofuran acceptor was more temperature resistant than the initial form of photochromes with a tricyanopyrrole acceptor.
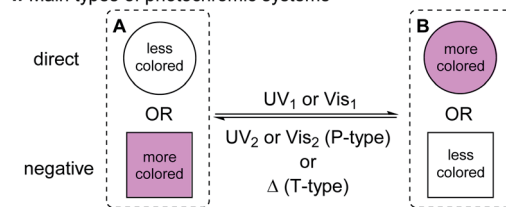
1 Introduction

Photochromic compounds are an intensively studied group of molecules due to their wide range of practical application. They are used in optically functionalized organic field-effect transistors (OFET)[1] and nanosystems,[2] and as multiaddressable architectures,[3] solar thermal fuels,[4] fluorophores at the molecular and nanoparticle levels,[5] and all-visible-light-triggered materials[6] as well as in biological research.[7–9]

Ultraviolet or visible light irradiation causes a reversible transformation of photochromes **A** into a metastable photoinduced form **B** (Fig. 1). It should be noted that studies of photochromes with the possibility to use visible light only[6] as a non-destructive and selective trigger to control the properties of substances and materials are intensified nowadays. Depending on a chromaticity of transformations direct and negative photochromism are distinguished. In the first case, the initial form **A** absorbs shorter wavelengths than photoinduced form **B** which is generally deeply colored. In contrary, for the negative photochromes the initial form **A** absorbs longer wavelengths, and the form **B** is less colored or completely colorless. It has been noted[10,11] that negative photochromes are much less common and therefore poorly studied.
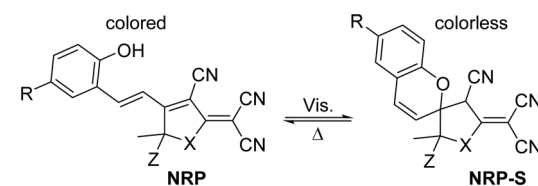
The photoinduced form **B** can be stable during a long period at dark conditions (P-type photochromism), or it spontaneously returns to the initial state **A** at room or raised temperature (T-type photochromism).[12–14] In the case of T-type photochromes,

this feature is important and exciting because it allows to control the stability of the photoinduced form by changing the temperature conditions. This issue has been well studied for
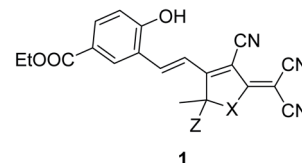

Fig. 1 Known photochromic systems and the object of the presented work.

Ulyanov Chuvash State University, Moskovsky pr., 15, Cheboksary, Russia 428015. E-mail: belikovmil@mail.ru

known groups of photochromes, such as spiropyrans,[15,16] spirooxazines,[17] azobenzenes,[18,19] diarylethenes,[20,21] dihydropyrene,[22] dihydroindolizines[23] and bindone derivatives.[24]

Papers[15–24] also demonstrate that the analysis of the temperature effect on the rate constant allows to estimate various important energy parameters of the reverse thermal reaction of photochromes, for example activation energy.

Compounds bearing a nitrile-rich acceptor and δ-OH-group in the same molecule are a relatively poorly studied group of negative photochromes (**NRP**, Fig. 1).[25–31]

NRP derivatives show photochromism under irradiation by visible light. Their colored initial form is converted into a colorless spiran **NRP-S**. The reverse reaction occurs when the solutions is stored in the dark, characterizing **NRP** derivatives as T-type photochromes. The importance of a more detailed study of this group of photochromes is supported by the fact that the possibility for photo-regulation of acidic[25,26] and fluorescent[27] properties of some representatives has been reported, that indicates the prospects of their practical application.

It should be noted that, despite the reported data on the T-type photochromism of **NPR** structures, there is no information in the literature about the temperature effect on the process of dark thermal relaxation of the photoinduced **NRP-S** form. Therefore, the thermodynamic parameters of this process are also unknown. Thus, the aim of this work is to investigate the influence of temperature on the dark reaction rate of photochromes **1**, as well as to obtain the data on the thermal stability of **NRP** photochromes in an individual form.

2   Results and discussion

2.1   Synthesis and structure determination

To investigate temperature effect on the stability of the photo-induced form of **NRP** derivatives, it was necessary to select a convenient model object whose dark reverse reaction rate was easy to register both at decreased and raised temperature. We used our reported correlation between the Hammett constants σ^+ for the substituent in the aryl ring and the observed half-lives ($\tau_{1/2}$) of the photoinduced **NRP-S** form.[28] According to these data, electron-donating and halogen substituents caused rather small $\tau_{1/2}$ values at room temperature, and electron-withdrawing groups slowed down the dark reaction. Thus, we chose photochrome **1a** bearing an ester group in the phenolic ring as the most convenient object. The half-life period of the photoinduced **NRP-S** form of this compound was about 85
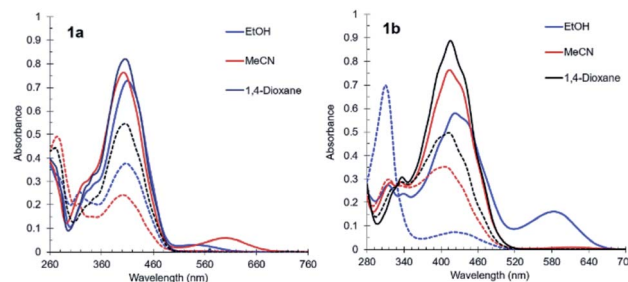

Fig. 2 UV-Vis spectra of compounds **1a** and **1b** in ethanol (blue), acetonitrile (red) and 1,4-dioxane (black) before (solid line) and after (dashed line) visible light irradiation for 1 min ($C = 2.5 \times 10^{-5}$ M, 20 °C).

seconds in ethanol at room temperature, that was considered as convenient for further investigations.

Also, a previously undescribed compound **1b**, bearing a furan ring in the structure as a nitrile-rich heterocyclic unit, was chosen as a second study object. The synthesis of these two compounds **1** was based on the interaction of the corresponding tricyano-substituted acceptors **2a** and **2b** with ethyl 3-formyl-4-hydroxybenzoate in ethanol in the presence of ammonium acetate under an argon atmosphere (Scheme 1) giving 62–76% isolated yield. Structure of compounds **1** was supported with IR-, NMR spectroscopy and mass-spectrometry.

2.2   Investigation of the photochromic properties

Investigation of the temperature effect on the rate of dark reaction of photochromes **1** was carried out using UV-Vis spectroscopy. The absorption spectra of compounds **1** were registered in different solvents as ethanol, acetonitrile and 1,4-dioxane. Fig. 2 shows the absorption spectra of **NRP 1a,b** before and after irradiation by visible light at 20 °C. The absorption spectra are characterized with intense bands in the visible region centered in the range of 404–410 nm for pyrrole **1a** and 414–424 nm for furan **1b**. There is also a second small band in the longer wavelength region of the spectrum in the range of 535–602 nm, corresponding to the quinoid form of compounds **1**.

Fig. 2 shows that after visible light irradiation an absorption band in the visible region is decreased indicating a negative photochromic process for compounds **1** in each solvent (Table 1).

Depending on the solvent, the photoconversion of the initial form **1** into the photoinduced one is different, for example, for
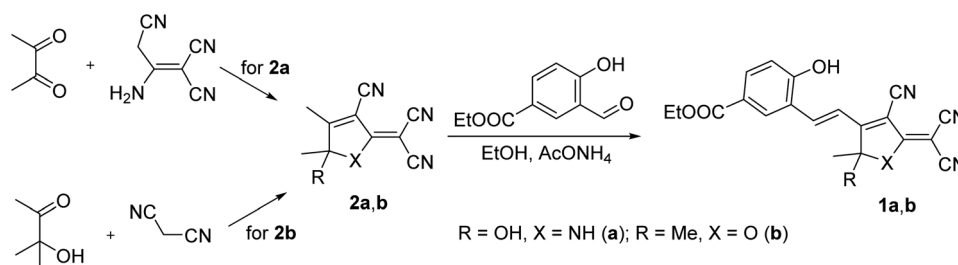

Scheme 1 Synthesis of compounds **1a,b**.

Table 1 Light absorption and photochromic characteristics of compounds **1a,b** at 20 °C

Compound	Solvent	λ_{abs}^{max} (nm)	$\varepsilon \times 10^4$ (L × mol^{-1} × cm^{-1})	Abs	Abs$_{PSS}$	PC^a (%)
1a	EtOH	410	2.92	0.730	0.376	48
		535	0.12	0.030	0.005	
	MeCN	404	3.05	0.762	0.241	68
		602	0.24	0.059	—	
	1,4-Dioxane	406	3.28	0.820	0.547	33
1b	EtOH	424	2.32	0.579	0.072	87
		583	0.64	0.160	—	
	MeCN	414	3.05	0.763	0.342	55
	1,4-Dioxane	415	3.54	0.886	0.494	44

^{a} Photoconversion percentage was estimated using decrease of the main absorption band.
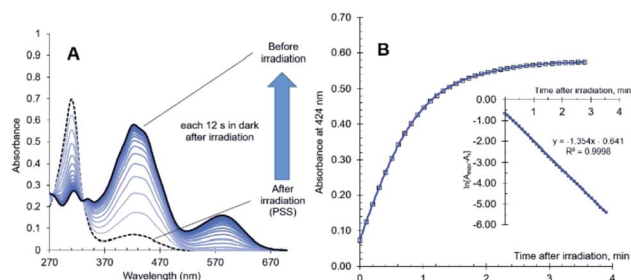
Fig. 3 UV-Vis spectra (A) and kinetics of the dark reverse reaction, λ_{abs} = 424 nm (B) of the compound **1b** before and after irradiation (EtOH, C = 2.5 × 10^{-5} M, 20 °C).

furan **1b** it changes from 87% in ethanol to 44% in 1,4-dioxane. Then, the absorption spectra of photochromes **1a,b** were registered at various temperatures in each of three solvents before and after irradiation. Fig. 3A shows the absorption spectra of compound **1b** in ethanol before and after irradiation in dynamics at 20 °C.

Fig. 3A shows that the intensity of the band at 424 nm was significantly decreased under irradiation by visible light. After the irradiation had been stopped, the solution was storing in dark conditions and the absorbance was gradually returning to the initial value. Fig. 3B shows first-order kinetics of the dark thermal transformation of compound **1b** after irradiation by visible light in ethanol.

2.3 Investigation of the temperature effect on the thermal relaxation of the photoinduced form

We observed that the rate of the dark reaction changes significantly depending on the temperature. For example, the half-life $\tau_{1/2}$ of the photo-induced form of pyrrole **1a** in ethanol could be changed by more than 15 times from 8.3 min to 0.5 min (Table 2) upon changing the temperature from 10 to 30 °C. A similar dependence in ethanol was observed for furan derivative **1b**.

Investigation of the temperature effect in 1,4-dioxane showed a significant difference in the rate of reverse reaction for compounds **1a** and **1b** (Fig. 4). Thus, the half-life period ($\tau_{1/2}$) of **1a** is 23.2 min and for furan **1b** it is 0.4 min only (Table 2) at

Table 2 Solvent and temperature effects on the rate of dark thermal reaction of the photoinduced form of compounds **1a,b**

Compound	Solvent	Temperature, T (°C)	Rate constant^a, k (min^{-1}) or (M × min^{-1})	Half-life period^b, $\tau_{1/2}$ (min)
1a	EtOH	10	0.083	8.3
		15	0.180	3.9
		20	0.351	2.0
		25	0.708	1.0
		30	1.381	0.5
	MeCN	10	0.38 × 10^{-6}	24.1
		15	0.76 × 10^{-6}	12.2
		20	1.46 × 10^{-6}	6.3
		25	2.79 × 10^{-6}	3.2
		30	4.98 × 10^{-6}	1.8
		35	8.95 × 10^{-6}	1.0
	1,4-Dioxane	35	0.009	75.7
		40	0.017	41.1
		45	0.030	23.2
		50	0.057	12.1
		55	0.102	6.8
		60	0.175	4.0
1b	EtOH	5	0.144	4.8
		10	0.296	2.3
		15	0.626	1.1
		20	1.354	0.5
		25	2.679	0.3
		30	4.947	0.2
		35	8.778	0.1
	MeCN	10	0.35 × 10^{-6}	19.7
		15	0.69 × 10^{-6}	10.1
		20	1.48 × 10^{-6}	4.7
		25	2.64 × 10^{-6}	2.7
		30	4.82 × 10^{-6}	1.6
		35	8.51 × 10^{-6}	0.9
	1,4-Dioxane	20	0.091	7.6
		25	0.182	3.8
		30	0.347	2.0
		35	0.624	1.1
		40	0.997	0.7
		45	1.792	0.4

^{a} For first-order reactions in ethanol and 1,4-dioxane (min^{-1}), for pseudo-zero order reactions in acetonitrile (M × min^{-1}). ^{b} The half-life period ($\tau_{1/2}$) was estimated as 0.693/k for first-order reactions in ethanol and 1,4-dioxane, and as $A_{PSS}/2k$ for pseudo-zero order reactions in acetonitrile.
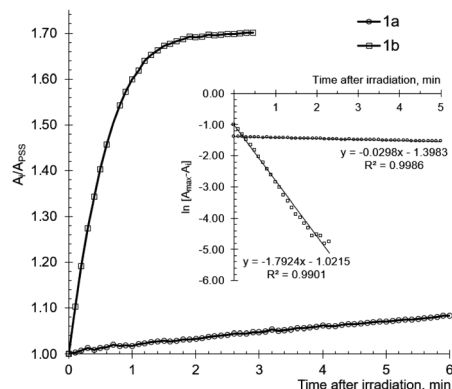
Fig. 4 Kinetics of the reverse thermal transformation for the compounds **1a** (circles) and **1b** (squares), the plot of fitting the concentration of photo-induced form in a first-order kinetic equation in 1,4-dioxane at 45 °C ($C = 2.5 \times 10^{-5}$ M).
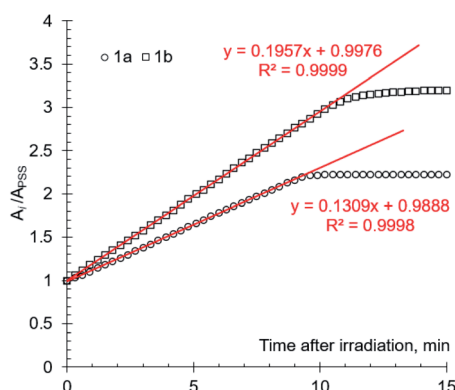

Fig. 5 Kinetics of the reverse thermal transformation of compound **1a** (circles) and **1b** (squares) in MeCN ($C = 2.5 \times 10^{-5}$ M, 20 °C).

45 °C. It should be noted, that kinetics of the reverse thermal reactions of photochromes **1a,b** in ethanol (Fig. 3B) and 1,4-dioxane (Fig. 4) were fitted to the first-order equation at each of the studied temperatures.

Acetonitrile solutions of compounds **1a,b** demonstrated a comparable with ethanol temperature effect on the rate of the dark reverse reaction. Thus, the half-life period ($\tau_{1/2}$) of furan derivative **1b** changes from 19.7 min to 1.6 min ranging the temperature from 10 to 30 °C (Table 2). At the same time, dark thermal reaction in acetonitrile fits to a pseudo-zero order
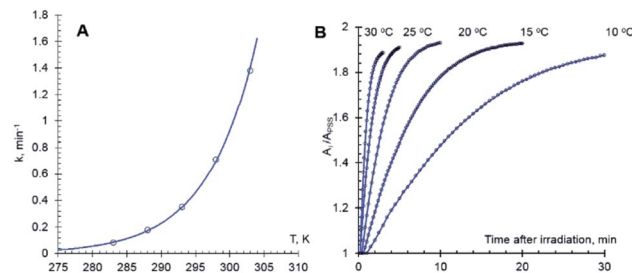

Fig. 6 Temperature effect on the rate constant of the dark thermal relaxation of compound **1a** in ethanol (A); absorbance changes of compound **1a** in ethanol after irradiation by visible light vs. time at various temperatures (B).

kinetic equation (Fig. 5) regardless the temperature and the type of heterocyclic unit of compounds **1**.

It is worth mentioning that pseudo-zero reaction order is usually not observed in solutions; therefore, the obtained data are rather unique example. Zero-order reactions are usually found for heterogeneous or enzyme catalyzed processes.[32–36] The presence of a rate-limiting step allowing only a small fraction of the reactant molecules to react is typical for such reactions. Thus, the reactant conversion occurs with constant rate and therefore the true reaction order is hidden.

In the case of compounds **1**, pseudo-zero reaction order is apparently caused by low deprotonation rate of the photoinduced CH-acid **1S** in acetonitrile (Scheme 2), since MeCN is a protonophobia solvent and poorly solvates anions.[37] In such solvent as acetonitrile deprotonation of the photoinduced CH-acid **1S** becomes a rate-limiting step of the dark reverse reaction unlike other solvents where the reaction rate directly associated with anion **1S⁻** concentration. Therefore, in acetonitrile deprotonation process is followed by the immediate consumption of **1S⁻** and the ring-opening occurs with a constant rate.

The discovery of novel zero-order processes is significant, because such a system could be used, for example, for prolonged drug delivery.[38,39]

2.4 Calculation of activation parameters for the thermal relaxation of the photoinduced form

The obtained data on the temperature effect on the dark thermal reaction rate of the photoinduced form of compounds **1** made it possible to estimate the activation energy and other thermodynamic parameters of this process for the first time.
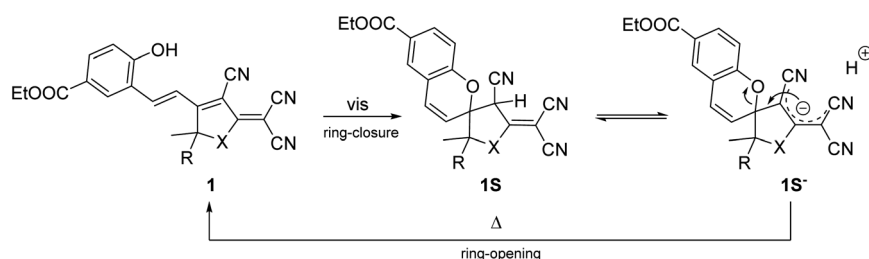
Scheme 2 A possible scheme of photochromic transformations of compounds **1a,b**.

Table 3 Thermodynamic parameters of the thermal relaxation of compounds **1a,b**

Comp.	Solvent	E_a (kJ mol^{-1})	$\Delta H^{\neq}$ (kJ mol^{-1})	$\Delta S^{\neq}$ (J K^{-1} mol^{-1})	A (s^{-1})
1a	EtOH	99.6	97.2	44.3	3.40×10^{15}
	1,4-Dioxane	101.4	98.7	2.2	2.37×10^{13}
1b	EtOH	98.8	96.4	52.3	8.95×10^{15}
	1,4-Dioxane	91.3	88.8	4.7	3.02×10^{13}

Fig. 6A demonstrates an exponential dependence of the reverse reaction rate constant on temperature. Fig. 6B also shows the relationship between the absorbance increasing rate of solution **1a** in ethanol after visible light irradiation and time at various temperatures.

The activation energy (E_a) and frequency factor (A) were calculated from the experimental dark reverse reaction rate constant k values by the Arrhenius equation (eqn (1)), where R is the universal gas constant and T is the absolute temperature. These obtained data are collected in the Table 3. The Arrhenius plot (Fig. 7A) shows a good correlation for both photochromes **1** in different solvents.

$$\ln k = \ln A - \frac{E_a}{RT} \quad (1)$$

The activation enthalpy ($\Delta H^{\neq}$) and the activation entropy ($\Delta S^{\neq}$) were calculated by the Eyring equation, where k_B and h are the Bolzmann and Planck constants, respectively.

$$\ln \frac{k}{T} = \frac{-\Delta H^{\neq}}{RT} + \ln \frac{k_B}{h} + \frac{\Delta S^{\neq}}{R} \quad (2)$$

Fig. 7B shows the Eyring plot with an excellent linearity. We have found that, depending on the solvent and type of the nitrile-rich heterocycle, the activation energy is in the range from 91.3 to 101.4 kJ mol^{-1} (Table 3). The activation enthalpy of the studying process is in the range of 88.8–98.7 kJ mol^{-1}. More significant differences have been found for the activation entropy values. For the dark reaction in ethanol $\Delta S^{\neq}$ is 44.3–52.3 J K^{-1} mol^{-1}, while in 1,4-dioxane it is much less, namely 2.2–4.7 J K^{-1} mol^{-1}. A similar dependence has been also shown for the frequency factor (A), it is significantly lower in 1,4-dioxane. The obtained A and $\Delta S^{\neq}$ values are consistent with the observed lower $\tau_{1/2}$ of photo-induced form in ethanol.

Data on acetonitrile solutions were not included in the calculations of activation parameters, because the kinetics of reverse thermal process fit to the pseudo-zero order equation and the observed rate constants are not comparable with rate constants of reactions occurred in ethanol and 1,4-dioxane.
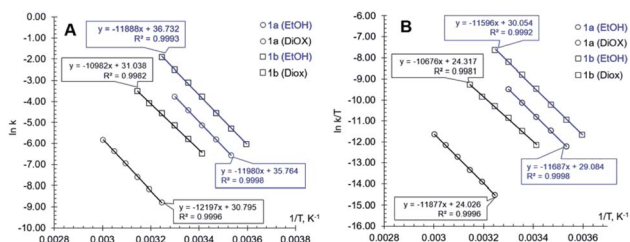
2.5 Thermal stability of the initial state in an individual form

A thermal stability of the initial state of **NRP** structures in an individual form is another completely unrevealed issue. This parameter is one of the most important ones for organic chromophores when they are considering for practical application. It demonstrates the acceptable temperature range for compound in which it can be used.

In this regard, we evaluated the thermal stability of the synthesized **NRP** derivatives **1a,b** using thermogravimetric analysis for the first time. It was found that furan **1b** did not undergo any significant changes upon heating up to 300 °C in an argon atmosphere. A weight loss of 10.4% occurred in the range of 300–320 °C which was accompanied by melting with decomposition (Fig. 8). Pyrrole **1a** showed lower thermal stability. It underwent a thermal decomposition in the range of 200–245 °C with a 6.2% weight loss. Such a difference of the TGA curves was probably associated with the presence of a labile aminoalcohol moiety in the structure of pyrrole **1a**.

Fig. 7 Arrhenius (A) and Eyring (B) plots for compounds **1a** (circles) and **1b** (squares) in ethanol (blue) and 1,4-dioxane (black) ($C = 2.5 \times 10^{-5}$ M).
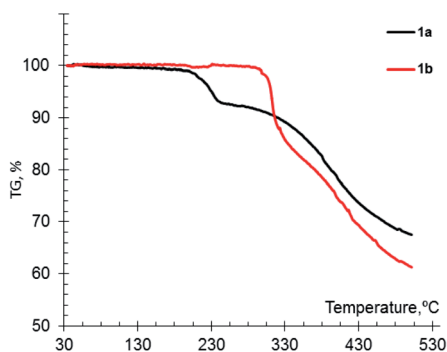
Fig. 8 TGA curves of compounds **1a** and **1b** at the heating rate of 10 °C min^{-1} under an argon atmosphere.

3 Experimental

3.1 Materials and methods

The progress of reactions and the purity of products were monitored by TLC on Sorbfil plates (spots were visualized under

UV light, by treatment with iodine vapor, or by heating). The IR spectra were recorded on an FSM-2201 spectrometer with Fourier transform from samples dispersed in mineral oil. The NMR spectra were measured in DMSO-d_6 on Bruker DRX-500 spectrometer using tetramethylsilane as an internal reference. Elemental analyses were performed using a FlashEA 1112 CHN analyzer. The mass spectra were obtained on a mass spectrometer Finnigan MAT INCOS-50. The UV spectra were recorded on an Agilent Cary 60 UV-Vis Spectrophotometer. Kinetic data of the dark thermal reaction were recorded at different thermostat temperatures using Peltier cell holder accessory. To study the photochromic behavior of compounds, the solutions were irradiated with non-filtered visible light by LED XM-LT6 CREE (spectral range of 400–700 nm, a luminous power density equal to 205 mW cm^{-2}). Thermogravimetric analysis was performed on a simultaneous thermogravimetry/differential thermal analyzer Shimadzu DTG-60. The syntheses of the starting compounds **2a,b** were carried out according to the described procedures.[40,41]

3.2 Synthesis of ethyl (*E*)-3-(2-(4-cyano-5-(dicyanomethylene)-2,2-dimethyl-2,5-dihydrofuran-3-yl)vinyl)-4-hydroxybenzoate 1b

0.194 g (1 mmol) of ethyl 3-formyl-4-hydroxybenzoate and 77 mg (1 mmol) of ammonium acetate were added to a suspension of 0.199 g (1 mmol) of TCF in 3 mL of 96% ethanol under argon atmosphere. The resulting mixture was stirred at room temperature for 10 h until the complete consumption of TCF monitored by TLC. The obtained solid product was filtered off, washed 3 times by 2 mL of ethanol and then dried in a vacuum drying cabinet (1 torr) over $CaCl_2$ for 3 days.

3.3 Spectral characterization of compounds 1b

Yellow solid; mp 311–312 °C (dec.); yield 76%. IR (mineral oil, ν, cm^{-1}): 3305 (OH), 2230, 2214 (C≡N), 1694 (C=O), 1589 (C=C), 1279 (CO). ^{1}H NMR (500.13 MHz, DMSO-d_6) δ: 1.32 (3H, t, $J = 7.1$ Hz, OCH$_2$CH$_3$), 1.81 (6H, s, 2CH$_3$), 4.31 (2H, t, $J = 7.1$ Hz, OCH$_2$CH$_3$), 7.05 (1H, d, $J = 8.6$ Hz, C$_6$H$_3$), 7.64 (1H, d, $J = 16.5$ Hz, CH =), 7.93 (1H, dd, $J = 2.2, 8.6$ Hz, C$_6$H$_3$), 8.07 (1H, d, $J = 16.5$ Hz, CH =), 8.42 (1H, d, $J = 2.2$, Hz, C$_6$H$_3$), 11.83 (1H, s, OH). ^{13}C NMR (125.76 MHz, DMSO-d_6) δ: 14.32, 25.29, 54.25, 60.59, 99.10, 99.33, 111.02, 111.91, 112.74, 116.77, 117.04, 121.33, 121.53, 133.65, 134.21, 143.63, 162.25, 165.11, 176.31, 177.08. MS, (EI, 70 eV): *m/z* (%) 375 [M]$^+$ (48), 360 [M–Me]$^+$ (22), 290 (100). Anal. calcd for C$_{21}$H$_{17}$N$_3$O$_4$: C, 67.19; H, 4.56; N, 11.19. Found: C, 67.01; H, 4.66; N, 11.04.

4 Conclusions

Thus, visible-light-sensitive representatives of **NRP** photochromes bearing an ester group were synthesized. The temperature effect on the rate of thermal relaxation of the photoinduced form in various solvents was described for the first time for these compounds. Regardless the temperature the first order kinetics of the reverse thermal reaction was observed in ethanol and 1,4-dioxane, while an unusual pseudo-zero

kinetics was registered in acetonitrile solution. Using the Arrhenius and Eyring equations the activation energy of this process as well as the thermodynamic parameters, such as entropy and enthalpy of the activation were calculated. A higher temperature stability of the initial state of the furan derivative in an individual form was shown in comparison with pyrrole containing **NRP**. The obtained data indicated wide possibilities for varying the thermal stability of **NRP** derivatives by changing both the structure of the photochrome and the used solvent.

Conflicts of interest

There are no conflicts to declare.

Acknowledgements

Notes and references

1 Y. Wakayama, R. Hayakawa, K. Higashiguchi and K. Matsuda, *J. Mater. Chem. C*, 2020, **8**, 10956.
2 L. Wang and Q. Li, *Chem. Soc. Rev.*, 2018, **47**, 1044.
3 H. Nie, J. L. Self, A. S. Kuenstler, R. C. Hayward and J. Read de Alaniz, *Adv. Opt. Mater.*, 2019, **7**, 1900224.
4 L. Dong, Y. Feng, L. Wang and W. Feng, *Chem. Soc. Rev.*, 2018, **47**, 7339.
5 T. Fukaminato, S. Ishida and R. Métivier, *NPG Asia Mater.*, 2018, **10**, 859.
6 Z. Li, C. He, Z. Lu, P. Li and Y.-P. Zhu, *Dyes Pigm.*, 2020, **182**, 108623.
7 Z. L. Pianowski, *Chem.–Eur. J.*, 2019, **25**, 5128.
8 H. Cheng, J. Yoon and H. Tian, *Coord. Chem. Rev.*, 2018, **372**, 66.
9 S. Jia, W.-K. Fong, B. Graham and B. J. Boyd, *Chem. Mater.*, 2018, **30**, 2873.
10 S. Aiken, R. J. L. Edgar, C. D. Gabbutt, B. M. Heron and P. A. Hobson, *Dyes Pigm.*, 2018, **149**, 92.
11 V. A. Barachevsky, *Rev. J. Chem.*, 2017, **7**, 334.
12 M. Kathan and S. Hecht, *Chem. Soc. Rev.*, 2017, **46**, 5536.
13 V. Kumar Gupta, in *Dyes Pigm.*, [Working Title], IntechOpen, 2021.
14 A. Bianco, S. Perissinotto, M. Garbugli, G. Lanzani and C. Bertarelli, *Laser Photonics Rev.*, 2011, **5**, 711.
15 H. Görner, *Phys. Chem. Chem. Phys.*, 2001, **3**, 416.
16 M. Zanoni, S. Coleman, K. J. Fraser, R. Byrne, K. Wagner, S. Gambhir, D. L. Officer, G. G. Wallace and D. Diamond, *Phys. Chem. Chem. Phys.*, 2012, **14**, 9112.
17 J. Liu, A. K.-W. Chan, M. Ng, E. Y.-H. Hong, N. M.-W. Wu, L. Wu and V. W.-W. Yam, *Organometallics*, 2019, **38**, 3542.
18 D. L. Isac, A. Airinei, M. Homocianu, N. Fifere, C. Cojocaru and C. Hulubei, *J. Photochem. Photobiol., A*, 2020, **390**, 112300.
19 G. Angelini, C. Campestre, L. Scotti and C. Gasbarri, *Molecules*, 2017, **22**, 1273.

20 D. Kitagawa, T. Nakahama, Y. Nakai and S. Kobatake, *J. Mater. Chem. C*, 2019, **7**, 2865.

21 K. Inaba, R. Iwai, M. Morimoto and M. Irie, *Photochem. Photobiol. Sci.*, 2019, **18**, 2136.

22 K. Ayub and R. H. Mitchell, *J. Org. Chem.*, 2014, **79**, 664.

23 S. A. Ahmed, N. El Guesmi, B. H. Asghar, F. Maurel, I. I. Althagafi, K. S. Khairou and H. A. Muathen, *J. Phys. Org. Chem.*, 2016, **30**, e3614.

24 V. Lokshin, L. Bekere and V. Khodorkovsky, *Dyes Pigm.*, 2017, **145**, 570.

25 V. K. Johns, P. Peng, J. DeJesus, Z. Wang and Y. Liao, *Chem.– Eur. J.*, 2014, **20**, 689.

26 C. Yang, T. Khalil and Y. Liao, *RSC Adv.*, 2016, **6**, 85420.

27 M. Yu. Belikov, M. Yu. Ievlev, S. V. Fedoseev and O. V. Ershov, *New J. Chem.*, 2020, **44**, 6121.

28 M. Yu. Belikov, M. Yu. Ievlev, S. V. Fedoseev and O. V. Ershov, *Res. Chem. Intermed.*, 2020, **46**, 3477.

29 M. Yu. Belikov, M. Yu. Ievlev, S. V. Fedoseev and O. V. Ershov, *New J. Chem.*, 2019, **43**, 8414.

30 M. Yu. Belikov, M. Yu. Ievlev, S. V. Fedoseev and O. V. Ershov, *Res. Chem. Intermed.*, 2019, **45**, 4625.

31 M. Yu. Belikov, S. V. Fedoseev, M. Yu. Ievlev, O. V. Ershov, K. V. Lipin and V. A. Tafeenko, *Synth. Commun.*, 2020, **50**, 2413.

32 Y. Chen and Y.-F. Song, *ChemPlusChem*, 2013, **79**, 304.

33 J. P. Lopes, S. S. S. Cardoso and A. E. Rodrigues, *AIChE J.*, 2009, **55**, 2686.

34 G. R. Warner, Y. Somasundar, C. Weng, M. H. Akin, A. D. Ryabov and T. J. Collins, *Chem.–Eur. J.*, 2020, **26**, 7631.

35 D. Yu. Murzin, *Catal. Commun.*, 2008, **9**, 1815.

36 Y. Ji, Y. Shi, Y. Yang, P. Yang, L. Wang, J. Lu, J. Li, L. Zhou, C. Ferronato and J.-M. Chovelon, *J. Hazard. Mater.*, 2019, **361**, 152.

37 J. F. Coetzee, in *Progress in Physical Organic Chemistry*, John Wiley & Sons, Inc., 2007, pp. 45–92.

38 M.-L. Laracuente, M. H. Yu and K. J. McHugh, *J. Controlled Release*, 2020, **327**, 834.

39 Y. Li, Y. Liu, R. Ma, Y. Xu, Y. Zhang, B. Li, Y. An and L. Shi, *ACS Appl. Mater. Interfaces*, 2017, **9**, 13056.

40 W. E. Moerner, R. J. Twieg, D. W. Kline and M. He, *US Pat.*, 134737, 2007.

41 M. Yu. Belikov, S. V. Fedoseev, M. Yu. Ievlev and O. V. Ershov, *Synth. Commun.*, 2018, **48**, 2850.